Imaging Normal Faults in Alluvial Fans using Geophysical Techniques: Field Example from the Coast of Gulf of Aqaba, Saudi Arabia

Sherif M. Hanafy[(1)], Sigurjon Jonsson[(1)], and Yann Klinger[(2)]*
1 King Abdullah University of Science and Technology (KAUST),
2 Institut de Physique du Globe – CNRS, Paris, France.

Summary

In this work we use geophysical methods to locate and characterize active faults in alluvial sediments. Since only subtle material and velocity contrasts are expected across the faults, we used seismic refraction tomography and 2D resistivity imaging to locate the fault. One seismic profile and one 2D resistivity profile are collected at an alluvial fan on the Gulf of Aqaba coast in Saudi Arabia. The collected data are inverted to generate the traveltime tomogram and the electric resistivity tomogram (ERT). A low velocity anomaly is shown on the traveltime tomogram indicates the colluvial wedge associated with the fault. The location of the fault is shown on the ERT as a vertical high resistivity anomaly.

Introduction

Alluvial fans and river terraces are classic geomorphological markers used to quantify deformation associated with active faults. Capability of rivers to incise, transport, or deposit sediments is very sensitive to small changes in river slope, making fluvial landforms a good proxy for vertical deformation. Lateral offset of alluvial fans and river terraces can also be used to decipher strike-slip motion along an active fault. In arid environment, such as the Gulf of Aqaba, erosion rate is low and landforms are preserved for a long time, allowing studying cumulative deformation over time periods exceeding many earthquake cycles. When combined with dating, measurements of cumulative deformation of alluvial morphology can then be used to determine deformation rate for the active tectonic structures of interest (e.g. Le Béon et al., 2010). In most cases, however, the incremental step in deformation, i.e. the deformation related to one earthquake, is missing and one is left only with cumulative deformation. In addition the geometry at depth of the fault structure is generally unknown, making long-term deformation extrapolation difficult. Using geophysical methods to determine such geometry of an active fault located in alluvial sediments is far from straight forward, as only subtle material and velocity contrasts are expected across the faults. Here, using the unique opportunity of having a partially preserved co-seismic rupture across alluvial sediments that can be used as a benchmark, we test different geophysical methods to investigate whether or not we can locate and characterize a known fault within an alluvial fan on the Gulf of Aqaba coast in Saudi Arabia.

Gulf of Aqaba marks the southern end of the Dead Sea (Levant) left-lateral transform fault. This ~1000km long fault system marks the western boundary of the Arabian plate and extends from the Red Sea, through Gulf of Aqaba, and north through the Dead Sea, Lebanon and Syria. The fault has been active for 15 My years and has a total displacement of about 107 km, representing an average slip rate of 5 mm/year during the Holocene (Klinger et al., 2000; Le Béon et al., 2008, 2010). The Gulf of Aqaba, about 180 km long and 25 km wide, is formed by a succession of 3 main faults segments that delimitate pull-apart basins. Normal faults associated with these basins accommodate some extension, in addition to the dominant strike-slip motion, giving way to an abrupt topography, which tops at about 2000 m asl in Sinai with the deepest basin being at 1800 m bsl. These basins are connected by en echelon strike-slip faults, trending N20E (Ben-Avraham, 1985). The extension and subsidence in the gulf has led to formation of extensive alluvial fans along the coastline of the gulf, particularly on its eastern side in Saudi Arabia.

The largest instrumental earthquake along the Dead Sea strike-slip fault in the recent past occurred on 22 Nov. 1995 within the Gulf of Aqaba (Klinger at al., 1999). The magnitude *Mw*7.3 earthquake caused about 30 injuries and 8 deaths on both the Saudi and the Egyptian sides of the Gulf. The main towns and cities affected by the earthquake were Nuweiba in Egypt, Eilat in Israel, Haql in Saudi Arabia, and Aqaba in Jordan. About thousand aftershocks were recorded following the mainshock in November and December 1995 (Klinger et al., 1999), some as large as *Mw* 5.0. The aftershock locations form two clusters in the northern part of the gulf, about 70 km apart, which likely correspond to the ends of the primary earthquake rupture located slightly off the Saudi Arabian coast (Klinger et al., 1999).

While the main rupture associated to the 1995 earthquake is located offshore, significant surface ruptures were found both on the Egyptian and Saudi Arabian coasts. The main surface cracks in Egypt were found north of Nuweiba and extend about 1 km, but they are thought to be mostly lateral spreading associated with seaward motion of the beach platform due to intense shaking during the earthquake (Klinger et al. 1999). The surface ruptures along the Saudi coastline are more extensive and extend for about 10-15 km within the alluvial fan deposits about 20 km south of Haql.

DOI http://dx.doi.org/10.1190/segam2014-1007.1

The ruptures occur on several overlapping segments along the coast, clearly reactivating older faults in many places and exhibiting normal faulting displacement that exceeds 10s of cm at some locations. Unlike on the Egyptian coast, the geometry of these cracks is oblique to the coast and underline structural directions that can be tight to the tectonic structure of the Gulf of Aqaba. In addition, in many places cumulative deformation such as uplifted terraces indicate that ruptures already occurred in a similar fashion in the past. Hence, as already suggested earlier, these surface ruptures might be parts of the primary faulting of the earthquake (Angelier et al., 1996).

Study Area and Fieldwork

The Saudi Arabian coast of Gulf of Aqaba is ideal to test to what extent we can locate and characterize faults in alluvial fans with geophysical methods. This is because many faults can easily be located on the surface, recent faulting has taken place, and then the area is easily accessible from the town of Haql. We therefore selected a study location in this area for a seismic and resistivity survey profile crossing one of these faults.

The study site is near the southern end of where fresh fault ruptures were found and both near the coast line and the main road south of Haql (Figures 1 and 2). The alluvial fans at this location extend about 6 km from the foot of the mountains (at ~300 m elevation) to the coastline. Uplifted terraces mark two roughly parallel normal faults near the coast (Figure 2c), with a 1995 related ground rupture located at the foot of the most western strand. We selected the profile location in one of the stream channels crossing the lower of these normal faults. The height of the terraces on each side of the profile is about 10 meters, which can be taken as a minimum value for the total displacement across the fault at this location. The offset of the 1995 rupture at this location is 10-20 cm (Figure 1).

The fieldwork was carried out in November 2013. The primary methods we employed to accurately track the location of the fault were seismic refraction traveltime tomography and 2D resistivity imaging, in hope to see contrasts and offsets related to the fault's locations. The study profile is about 300 m long, with 150 m to the west on the headwall of the fault and 150 meters to the east on the fault's footwall.

Data Acquisition and Processing

Two data sets were collected at the study site to map the subsurface structure along a profile across the known normal fault described above. The first data set is a seismic refraction data set and the second is a 2D resistivity imaging data set.

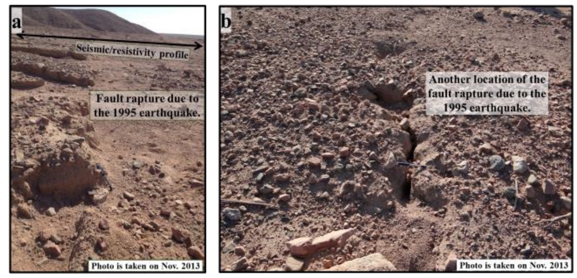

Figure 1: Two photos showing the fault rupture of the 1995 earthquake. The black line in (a) shows the location of the seismic/resistivity profiles across the fault.

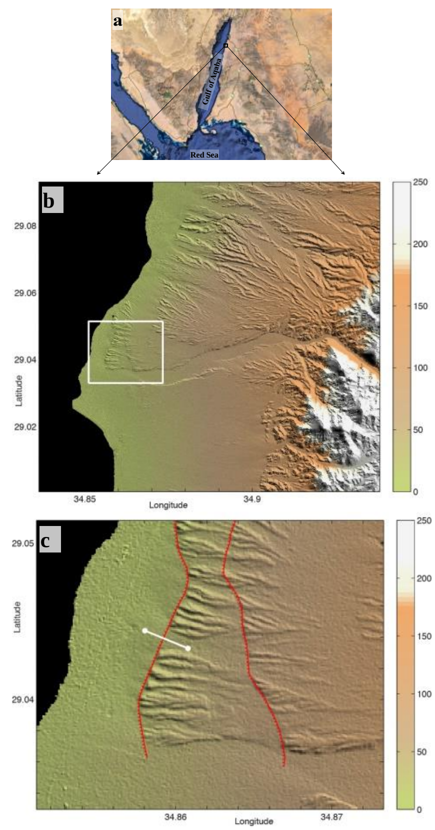

Figure 2: (a) A Google Earth satellite image showing the location of the study area at the eastern side of Gulf of Aqaba. (b) Shaded relief topographic map of the study area (colorscale in meters), with details shown in the lower panel (c), including the seismic/resistivity profile (white) and two easily identified normal faults (red). The white frame in (b) marks the location of the area shown in (c).

DOI http://dx.doi.org/10.1190/segam2014-1007.1

Seismic Refraction Data

A total of 120 common shot gathers were collected. Each shot gather has 120 traces at equal shot and receiver intervals of 2.5 m. The total length of the profile is 297.5 m (Figure 3). Data were recorded using a 1 ms sampling interval for a total recording time of 0.3 s. A 200 lb weight drop was used as the seismic source, with 10 to 15 stacks at each shot location. Figure 4 shows a shot gather example (CSG # 1), where the signal-to-noise ratio is high and first breaks of all traces are clear and can easily be picked.

The total number of recorded traveltimes are 14,400. We carried out a reciprocity test to eliminate unreliable traveltime picks, where the traveltime from a source at location A to a receiver at location B should equal to the traveltime from a source at location B to a receiver at location A. After the reciprocity test, 648 picks were rejected, while 13,752 picks remained for the inversion with a maximum source-receiver offset of 282.5 m.

First arrival traveltimes were inverted to generate a velocity tomogram of the subsurface (Figure 5a). The traveltime tomogram shows 3 layers:

- The first one is characterized by a P-wave velocity of 600-800 m/s and a thickness of 11 to 19 meters. The thickness of this layer gradually increases from the west to the east (Figure 5a).
- The second layer has a P-wave velocity of 1400 – 1600 m/s and thickness of 5 to 10 m.
- The third layer has higher P-wave velocities of over 2200 m/s and extend to the bottom of the tomogram.

A low velocity anomaly is shown between offsets 120 and 145 m, which is known as colluvial wedge and can be used as a good indication to the location of the fault (Buddensiek, 2007; Morey and Schuster, 1999; Nolan et al., 2011). The location of the active fault is visible on the tomogram at location X = 140 – 145 m, where the top of the second and third layers drops across the expected location of the fault. The depth to the third layer changes from about 31 m on the western side of the fault to about 23 m at the eastern side, indicating that the total fault offset may be about 8 m (Figure 5a).

The western side of the tomogram characterizes by a flat contact between the first and the second layer, while the eastern side characterizes by irregular first-second-layer contact especially between offsets 230 and 270 m. This could indicate the presence of another fault at the eastern side of the tomogram, however, more data is required to confirm this conclusion.

2D Resistivity Imaging

One 2D resistivity profile is acquired at the same location and parallel to the seismic profile. The acquisition parameters of the resistivity profile are:

- No. of nodes: 64
- Node interval: 5 m
- Configuration Array: Schlumberger-Wenner
- Total profile length: 315 m
- Both seismic and resistivity profiles share the same starting point at the western end of the profile

The collected data were inverted using the Res2DInv software to generate the resistivity tomogram (Ostrowski et al., 2010) shown in Figure (5b). Two distinct layers are visible in the resistivity tomogram, the first layer has resistivity values ranging from 400 to 500 Ohm.m to the west and from 250 to 400 Ohm.m to the east, with the layer thickness ranging between 6 and 10 m. The second layer extends to the bottom of the section and has low resistivity values ranging between 10 and 50 Ohm.m, except between offsets 130 and 145 m, where the resistivity values appear to increase to about 250 Ohm.m.

The location of the fault is shown on the resistivity tomogram as a vertical anomaly (between offsets 130 and 145 m) with higher resistivity values (250 Ohm.m) as shown in Figure 5b.

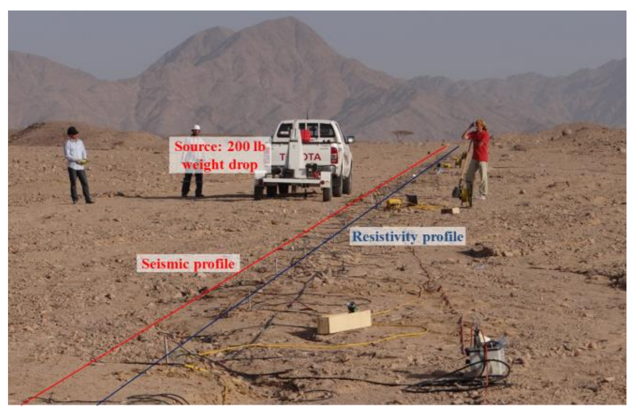

Figure 3: A photo taken during the data acquisition. Both the seismic (red line) and the resistivity (blue line) profiles are shown here. The photo is taken along the profile towards the east.

DOI http://dx.doi.org/10.1190/segam2014-1007.1

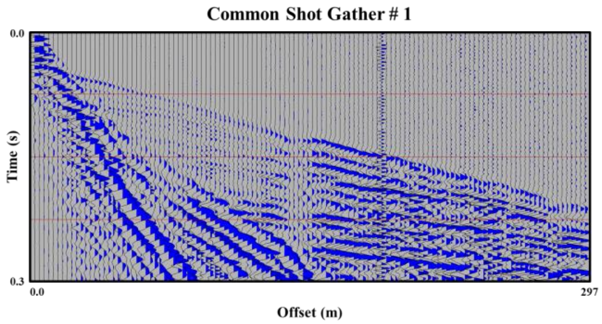

Figure 4: An example common shot gather, showing a high signal-to-noise ratio, with first arrivals that can easily be picked.

Conclusions

An active fault hidden in alluvial sediments at the Gulf of Aqaba, Saudi Arabia is located and characterized using surface geophysical techniques. Both seismic refraction traveltime tomography and electric resistivity imaging are used to locate the fault.

The traveltime and resistivity tomograms show some similarities and differences that can be summarized in the following points:

- The lateral location of the fault from both seismic and resistivity measurements coincides
- The total fault offset measured from the traveltime tomogram is 8 m.
- The first layer in the traveltime tomogram is thicker than that in the resistivity tomogram. A possible explanation to this inconsistence in the first-layer-thickness could be due to the fact that velocity tomogram mainly reflects lithology changes, while resistivity tomogram mainly reflects the fluid content.

The traveltime tomogram shows some indication of the existence of another fault at the eastern side of the section, while resistivity tomogram does not support this conclusion. One or more seismic/resistivity profiles are needed at the eastern side of the study area to further investigate the possibility of the existence of another fault.

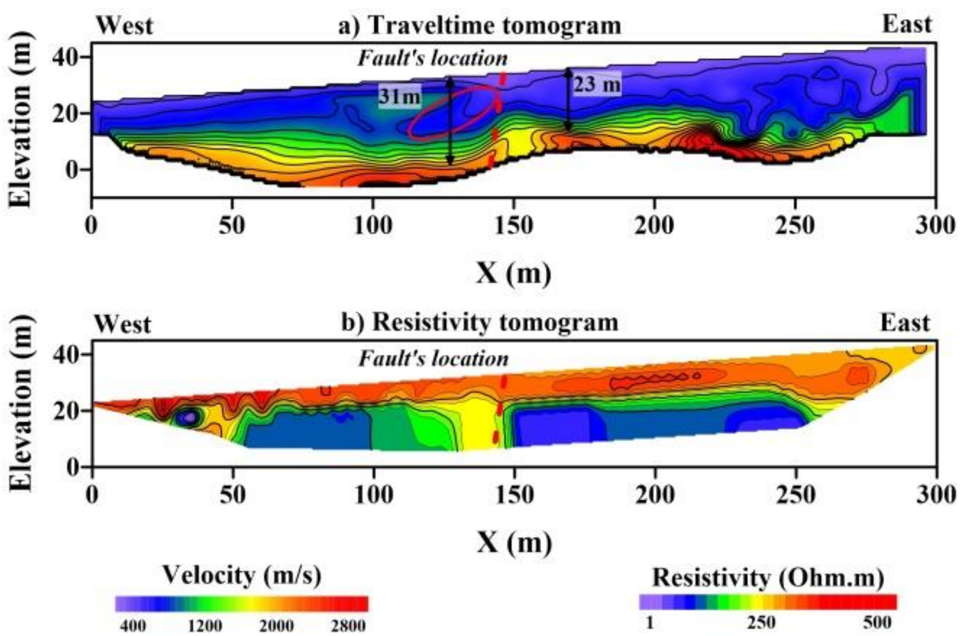

Figure 5: a) The seismic travel-time tomogram and b) the resistivity tomogram. The red-dashed line shows the suggested location of the fault, extrapolated from the fault's location at the surface. The red-solid ellipse shows a low-velocity region within the tomogram, which might be interpreted as a colluvial wedge associated with the fault.

DOI http://dx.doi.org/10.1190/segam2014-1007.1

http://dx.doi.org/10.1190/segam2014-1007.1

EDITED REFERENCES

Note: This reference list is a copy-edited version of the reference list submitted by the author. Reference lists for the 2014 SEG Technical Program Expanded Abstracts have been copy edited so that references provided with the online metadata for each paper will achieve a high degree of linking to cited sources that appear on the Web.

REFERENCES

Angelier, J., P. Hancock, M. Al-Dail, and N. Sha'at, 1996, Etude seismotectonique de failles actives entre Haql et Maqnah, Arabie Saoudite: Trace du séisme du Golfe d'Aqaba: 16th RST.

Ben-Avrahma, Z., 1985, Structural framework of the gulf of Elat (Aqaba), northern Red Sea: Journal of Geophysical Research, **90**, no. B1, 703–726, http://dx.doi.org/10.1029/JB090iB01p00703.

Buddensiek, M. L., J. Sheng, T. Crosby, G. T. Schuster, R. L. Bruhn, and R. He, 2007, Colluvial wedge imaging using traveltime and waveform tomography along the Wasatch fault near Mapleton, Utah: Geophysical Journal International, **162**, 246.

Klinger, Y., J. P. Avouac, L. Dorbath, N. Abou Karaki, L. Dorbath, D. Bourles, and J. L. Reyss, 2000, Slip-rate on the Dead Sea transform fault in northern Araba valley (Jordan): Geophysical Journal International, **142**, no. 3, 755–768, http://dx.doi.org/10.1046/j.1365-246x.2000.00165.x.

Klinger, Y. L. Rivera, H. Haessler, and J.-C. Maurin, 1999, Active faulting in the Gulf of Aqaba: New knowledge from the Mw7.3 earthquake of 22 November 1995: Bulletin of the Seismological Society of America, **89**, 1025–1036.

Le Béon, M., Y. Klinger, M. Al-Qaryouti, A. S. Mériaux, R. C. Finkel, A. Elias, O. Mayyas, F. J. Ryerson, and P. Tapponnier, 2010, Early Holocene and Late Pleistocene slip rates of the southern Dead Sea Fault determined from 10Be cosmogenic dating of offset alluvial deposits: Journal of Geophysical Research, **115**, no. B11, B11414, http://dx.doi.org/10.1029/2009JB007198.

Le Béon, M., Y. Klinger, A. Q. Amrat, A. Agnon, L. Dorbath, G. Baer, J. C. Ruegg, O. Charade, and O. Mayyas, 2008, Slip rate and locking-depth from GPS profiles across the southern Dea Sea Transform: Journal of Geophysical Research, **113**, B11403, http://dx.doi.org/10.1029/2007JB005280.

Morey, D., and G. T. Schuster, 1999, Paleoseismicity of Oquirrh fault, Utah from shallow seismic tomography: Geophysical Journal International, **138**, no. 1, 25–35, http://dx.doi.org/10.1046/j.1365-246x.1999.00814.x.

Nolan, J., S. D. Sloan, S. W. Broadfoot, R. McKenna, and O. M. Metheny, 2011, Near-surface void identification using MASW and refraction tomography techniques: 81st Annual International Meeting, SEG, Expanded Abstracts, **30**, 1401–1405.

Ostrowski, S., M. Lasocki, and G. Pacanowski, 2010, Electric resistivity tomography as a tool in geological mapping: Presented at the 72nd Annual International Conference and Exhibition, EAGE.

DOI http://dx.doi.org/10.1190/segam2014-1007.1